

Optical Coherence Tomography Features of Active and Inactive Retinal Neovascularization in Proliferative Diabetic Retinopathy

Sara Vaz-Pereira, MD,^{1,3} Javier Zarranz-Ventura, MD, PhD, FEBO,^{1,4} Dawn A. Sim, FRCOphth,^{1,2} Pearse A. Keane, MD, FRCOphth,^{1,2} Rebecca Smith, BSc, RMIP,¹ Catherine A. Egan, MBBS, FRANZCO,¹ Adnan Tufail, MD, FRCOphth^{1,2}

¹Medical Retina Department, Moorfields Eye Hospital NHS Foundation Trust, London, United Kingdom

²National Institute of Health Research (NIHR) Biomedical Research Centre at Moorfields Eye Hospital NHS Foundation Trust and UCL Institute of Ophthalmology, London, United Kingdom

³Department of Ophthalmology, Hospital de Santa Maria, Lisbon, Portugal

⁴Vitreo-Retinal Unit, Institut Clinic d'Oftalmologia (ICOF), Hospital Clinic, Barcelona, Spain

Correspondence and reprint requests:

Adnan Tufail, Medical Retina Department, Moorfields Eye Hospital NHS Foundation Trust, 162 City Road, London EC1V 2PD, United Kingdom.

Email: adnan.tufail@moorfields.nhs.uk

Disclosure:

Drs. Keane, Egan, Sim and Tufail have received a proportion of their funding from the Department of Health's NIHR Biomedical Research Centre for Ophthalmology at Moorfields Eye Hospital and UCL Institute of Ophthalmology. The views expressed in the publication are those of the author and not necessarily those of the Department of Health.

Dr. Sim has received funding from Fight For Sight UK, Grant 1987.

Dr. Zarranz-Ventura is a grant recipient of the Spanish Retina & Vitreous Society (Sociedad Española de Retina y Vitreo, SERV).

Drs. Sim, Zarranz-Ventura, and Keane have received travel grants from the Allergan European Retina Panel.

Dr. Tufail has been on advisory boards for Novartis, Pfizer, GSK, Thrombogenics, Bayer and Allergan.

Dr Vaz-Pereira has received consultant fees from Novartis and Bayer and has received travel grants from Alcon and Allergan.

Miss Smith has no disclosures to report.

The authors have no proprietary interest in the contents presented.

Running Head:

SD-OCT features of new vessels in PDR

Keywords:

Diabetes mellitus

Diabetic retinopathy

Neovascularization of the disc

Retinal neovascularization

Spectral domain optical coherence tomography

Summary Statement: Qualitative analysis of SD-OCT scans of retinal neovascularization in proliferative diabetic retinopathy identified 5 distinct signs of disease activity: presence of hyperreflective dots in the vitreous, epiretinal membrane, inner retinal tissue contracture, vitreous invasion and protrusion towards vitreous.

Word Count:

4757

Figures:

3

Tables:

3

Abbreviations:

DD – disc diameter

DM – diabetes mellitus

FA – fluorescein angiography

NVC – new vessel complexes

NVD – neovascularization of the disc

NVE – neovascularization elsewhere

PDR – proliferative diabetic retinopathy

SD-OCT – spectral domain optical coherence tomography

DRS – Diabetic Retinopathy Study

ETDRS – Early Treatment Diabetic Retinopathy Study

PVD – posterior vitreous detachment

ILM – internal limiting membrane

ERM – epiretinal membrane

UK NSC – United Kingdom National Screening Committee

CMT – central macular thickness

Abstract:

Purpose: To describe spectral domain optical coherence tomography (SD-OCT) features of retinal neovascularization in proliferative diabetic retinopathy (PDR) and thus to identify novel signs of new vessel activity.

Methods: Retrospective, cross-sectional study. Data were collected over a nine-month period. SD-OCT scans were performed over areas of new vessel complexes (NVC) in both the disc (NVD) and elsewhere (NVE), and were qualitatively graded by two masked observers. NVC activity was determined using clinical and angiographic criteria and correlated with SD-OCT features.

Results: 43 eyes of 30 patients with PDR were included. 61 NVC lesions (NVD-37.7%, NVE-62.3%) were captured by SD-OCT and analyzed. 63.9% were classified as active and 36.1% as quiescent. Five distinctive features were identified as significantly different between active and quiescent NVC: presence of vitreous hyperreflective dots in active NVC ($p=0.002$) and presence of epiretinal membrane ($p=0.04$), inner retinal tissue contracture ($p=0.03$), vitreous invasion ($p=0.02$) and protrusion towards vitreous ($p=0.002$) in quiescent NVC.

Conclusions: In this exploratory study, the presence of vitreous hyperreflective dots, epiretinal membrane, inner retinal tissue contracture, vitreous invasion and vitreous protrusion were identified as distinct signs of disease activity. Such parameters may be useful as a non-invasive imaging modality in eyes undergoing treatment for PDR.

Introduction:

Diabetic retinopathy, a microvascular complication of diabetes mellitus (DM),^{1,2} can be clinically classified as non-proliferative or proliferative diabetic retinopathy (PDR).^{3,4} PDR, which occurs in up to 50% in type 1, and 15% in type 2 diabetes, remains a major cause of visual disability.⁵ The classification of the new vessels depends on their location; neovascularization of the disc (NVD) if they are on the disc or within one disc diameter of the optic disc, or neovascularization elsewhere (NVE) if they are located more than one disc diameter from the disc margin.³

Optical coherence tomography (OCT), is a non-invasive imaging method⁶ that has changed how diabetic retinopathy is investigated, and has been widely adopted for the assessment of diabetic macular edema, both in clinical practice and clinical trials. It has also increased our understanding of how the disease affects the different layers of the retina and choroid, in particular, for the identification of retinal thickening, intra-retinal edema and changes of the vitreoretinal interface.⁷⁻¹⁰

Recently, it has been shown that it is possible to use spectral-domain OCT (SD-OCT) to evaluate the morphologic features of PDR. This could be useful in evaluating new vessel complexes (NVC) in their earliest stages, but also to identify associated vitreoretinal changes.¹¹ While NVD were first described as a hyperreflective lesion sitting over the optic disc or protruding from it, NVE were seen as flat vessels arising from the inner retina which then grew as hyperreflective loops.^{11,12} Adhesion and break through the posterior hyaloid, traction and vitreous invasion were also observed.^{11,12} Nevertheless, although SD-OCT is helpful in showing early and established NVC, while providing anatomic relationships and being in some cases more accurate than clinical examination or fluorescein

angiography, there is still limited evidence regarding the usefulness of this technique in determining disease activity.¹¹⁻¹⁴ Indeed, there have been no studies which address its potential to assess new vessel activity. In the landmark clinical trials of the Diabetic Retinopathy Study (DRS) and Early Treatment Diabetic Retinopathy Study (ETDRS), fluorescein angiography (FA) was used as an adjunct for the classification of disease severity, guiding laser therapy and evaluating the response to treatment.¹⁵⁻¹⁷ In large multicenter clinical trials, FA is usually not required, and performed at the investigator's discretion.¹⁸ In clinical practice however, it is often used to ascertain new vessel activity in the context of evaluating the response to treatment. As fluorescein angiography is an invasive procedure, it is not performed with the same frequency as SD-OCT. Identifying SD-OCT derived features of new vessel activity will enable the clinician to more closely monitor patients, and consequently tailor management decisions according to the individual's response to treatment – i.e., during a course of pan-retinal laser photocoagulation, or intravitreal pharmacotherapy.

In this study, we investigate the use of SD-OCT to describe features of retinal neovascularization in PDR, in an effort to identify novel signs of new vessel activity.

Material and Methods:

Inclusion Criteria and Data Collection:

Forty-three eyes of 30 non-consecutive patients with PDR, either with NVD or NVE, active or quiescent, as assessed by ophthalmoscopy according to the Early Treatment Diabetic Retinopathy Study (ETDRS) criteria were included.³ Clinical data collected included age, gender, disease type (type 1 and type 2 DM), best-corrected visual acuity (Snellen acuity charts), history of previous laser treatments and central macular thickness (CMT) in both eyes (Table 1). Patient demographic data, visual acuity and retinopathy grading were obtained from standardized electronic reports in the United Kingdom National Screening Committee (UK NSC) - Diabetic Eye Screening Programme, as described elsewhere.¹⁹ The baseline clinical characteristics of eyes included in the study are described in Table 2. Regarding NVC location, NVD were defined as complexes located in the disc or within 1DD from its margin, and NVE were defined as NVC located outside this area. NVC activity was ascertained using clinical examination, color fundus photographs and fluorescein angiography (FA).

Active NVC were considered to have a perfused blood column on fundoscopy and leakage seen in FA, while inactive NVC showed no red blood column present on fundoscopy and no obvious leakage in FA.³ Exclusion criteria included other causes of proliferative retinopathy such as retinal arterial and venous occlusion, ocular ischemic syndrome, radiation retinopathy or sickle cell retinopathy.

This data was collected over a nine-month period (May 2012 to January 2013) from medical retina clinics with a focus on diabetic eye disease at Moorfields Eye Hospital, London, United Kingdom and at the Department of Ophthalmology,

Hospital de Santa Maria, Lisbon, Portugal. Approval for data collection and analysis was obtained from the Moorfields Eye Hospital and Hospital de Santa Maria local ethics committee. This study was carried out according to the tenets set forth in the Declaration of Helsinki.

OCT Image Acquisition Protocol:

OCT images sets were obtained by experienced operators (B.S. and S.V.P.), using a standard, commercially available SD-OCT device (SPECTRALIS®, Heidelberg Engineering, Heidelberg, Germany). In each case, both macular and extramacular raster scan acquisition protocol were performed, centered on the fovea and the NVC respectively. SD-OCT images at the NVC were selected either with the vertical or horizontal scanning plane bisecting the NVC and the image sets size was adjusted accordingly in order to include the whole extent of the NVC, using equally spaced OCT B-scan sections, each composed of 50-100 averaged B-scans.

Qualitative analysis of OCT images:

All SD-OCT image sets were reviewed independently by two retina specialists (S.V.P. and D.A.S.) who were masked to the clinical information at the time of the assessment. Each image set was assessed for the presence of tomographic features which included vitreoretinal, retinal and NVC morphologic parameters (Table 3). Vitreoretinal parameters included 1) posterior vitreous detachment (PVD), defined as a detached posterior hyaloid seen as a thin hyperreflective layer above the internal limiting membrane (ILM); 2) thickening of the posterior hyaloid; 3) epiretinal membrane (ERM) in the area of the NVC, defined as a hyperreflective band anterior to the inner retinal surface, 4) presence of vitreoretinal traction with

retinal distortion; and 5) presence of hyperreflective dots in the vitreous cavity. 3D OCT maps were also evaluated in order to identify further vitreoretinal traction, such as tractional retinal detachment.

Retinal features included 1) evidence of retinal tissue contracture, seen as mechanical tractional changes at the NVC and surrounding retina causing distortion; 2) intra-retinal cysts identified as round or oval hyporeflective areas within the retina; and 3) retinal hyperreflective dots, seen as hyperreflective dots within the retinal layers. NVC parameters were graded according to 1) reflectivity of the NVC, being “medium” reflectivity if it was between the high reflectivity of the retinal pigment epithelium (RPE) and the hyporeflectivity from outer nuclear layer, and “high” if equal or greater in reflectivity than the RPE; 2) shadowing of the outer retina; 3) vitreous invasion, regarded as invasion through the posterior hyaloid / vitreous cavity; and 4) relative position of the NVC with regards to the retina (flat/protruding). In case of disagreement between graders, open adjudication was performed to obtain the final grading. A subset of images was then regraded at a later point to assess reproducibility.

Statistical Analysis:

Clinical and imaging data were analyzed with frequency and descriptive statistics. CMT was measured using the EDTRS foveal central subfield on macular SD-OCT. Snellen visual acuities were converted to logMAR visual acuities for the purposes of statistical analysis.

The Fisher’s exact test was used for statistical analysis of categorical variables in eyes with NVD, and the Chi-Squared test in eyes with NVE. The two-tailed t-test and the Mann-Whitney U test were used for continuous variables. Concordance between

graders for the qualitative SD-OCT features assessed was determined with κ index. For the strength of agreement range, we considered 0.21-0.40 to be fair agreement, 0.41-0.60 moderate agreement, 0.61-0.80 substantial agreement and 0.81-1.00 almost perfect agreement, as per previous suggested guidelines.²⁰ Results with a P value < 0.05 were considered statistically significant. Statistical analyses were performed using SPSS software version 16 (SPSS, Inc, Chicago, IL).

Results:

Baseline characteristics of patients and eyes analyzed:

The baseline demographics and clinical characteristics of the 30 patients included in the study are summarized in Table 1. The mean age was 55.6 years (Standard Deviation [SD]: 11.8) and 16 (53.3%) were male. Eight (26.7%) had type 1 and 22 (73.3%) had type 2 diabetes. Six patients (20%) had previous laser photocoagulation. Retinopathy grading was obtained from the standardized electronic reports as per the U.K. NSC with 10 (33.3%) patients being RP MP (diabetic retinopathy and maculopathy treated with laser) in both eyes, seven (23.3%) being RP M0 (diabetic retinopathy treated with laser and no maculopathy) in both eyes, two (6.7%) patients being bilaterally R3 M0 (PDR and no maculopathy), two (6.7%) patients graded bilaterally as R3 M1 (PDR with maculopathy), two (6.7%) patients being bilaterally RP M1 (diabetic retinopathy treated with laser and maculopathy) and seven (23.3%) patients having different grading between eyes. Disease activity was documented by clinical examination alone in 4 patients (13.3%), by additional color photographs in 7 patients (23.3%) and by fluorescein angiography in 19 patients (63.6%).

A total of 43 eyes were analyzed, 8 eyes had both NVD and NVE and 5 eyes had more than one focus of NVE. Four eyes had NVD and 8 eyes had NVE bilaterally. Mean logMAR visual acuity was 0.24 (SD: 0.19), 35 (81.4%) eyes had had previous laser panretinal photocoagulation at the time of the SD-OCT scan and the mean CMT was 311.3 μm (SD: 91.0). The mean age, sex, visual acuity and CMT did not differ significantly between eyes with active or quiescent new vessels (Table 2). A significant difference was observed regarding disease activity and the type of

diabetes and presence of previous laser treatment: most of the active eyes were of type 2 diabetics (77.8% vs 56.2%) and only 74% vs 93.8% had previous laser photocoagulation ($p=0.01$ and $p=0.001$, respectively).

Assessment of SD-OCT Features in New Vessel Complexes:

Sixty-one NVC were scanned, among which 23 (37.7%) were NVD and 38 (62.3%) NVE. All NVE were located posterior to equator with 13 (34.2%) being positioned inside the temporal arcades and 25 (65.8%) outside the arcades. The NVE were located in the superotemporal quadrant in 47.4% of cases, followed by the inferotemporal quadrant in 23.7%, the inferonasal quadrant in 21.1% and the superonasal quadrant in 7.9%. Active NVC represented 63.9% of the studied sample (39/61), whereas quiescent NVC included 36.1% (22/61). Regarding subgroups by NVC location and disease activity, 65.2% (15/23) of NVD and 63.2% (24/38) of NVE were active in the moment of the scan. All SD-OCT derived morphologic features of the NVD and NVE assessed are summarized in Table 3.

SD-OCT characteristics of NVC: Mostly of the scanned NVC revealed thickening of the posterior hyaloid (79.5% for active NVC, 45.5% for inactive NVC respectively) without signs of vitreoretinal traction (79.5%, 59.1%), no intraretinal cysts (76.9%, 63.6%) but presence of hyperreflective dots in the retina (66.7%, 54.5%), and no hyperreflective changes with regards to RPE layer (51.3%, 59.1%) but shadowing of the outer retinal layers (92.3%, 86.4%), without significant differences between active and inactive NVC.

Features of active versus inactive neovascularization at the disc (NVD):

Absence of posterior vitreous detachment was significantly more frequent in active NVD (93.3% vs 50%, 14/15 vs 4/8, $p=0.03$), however vitreous invasion was seen in

all quiescent cases (100%, 8/8) compared to active NVD complexes (40.0%, 6/15, $p=0.02$) (Figure 1). There were no significant differences in any of the other parameters evaluated.

Features of active versus inactive neovascularization elsewhere (NVE): The presence of hyperreflective dots in the vitreous overlying NVE was significantly more frequent in active NVE (70.8%, 17/24) than in quiescent NVE (21.4%, 3/14, $p=0.009$) (Figure 2a and Figure 3e-f). Active NVE sit flat on the retinal surface (66.7%, 16/24) (Figure 2a and Figure 3) significantly more than quiescent cases, which tended to protrude towards vitreous (85.7%, 12/14, $p=0.005$, Figure 2b-d). Both NVC presented with diverse shapes which included loops, C-shapes, funnel shape and a horizontal string. No other parameters were significantly associated with disease activity.

Shared features of active versus inactive NVD and NVE: A combined analysis of NVD and NVE complexes showed a significantly higher presence of hyperreflective dots in vitreous in active NVC (66.7%, 22/39) than in quiescent NVC (22.7%, 5/22) ($p=0.002$). The presence of ERM was more frequently observed in quiescent NVC (100%, 22/22) than in active NVC (76.9%, 30/39, $p=0.002$) (Figure 1 and Figure 2b-d), as was tissue contracture (77.3%, 17/22 vs 46.2%, 18/39, $p=0.04$). Vitreous invasion was more frequently observed in quiescent NVC (90.9%, 20/22) than active NVC (51.3%, 20/29, $p=0.02$), and indeed quiescent cases tended to protrude towards vitreous (86.4%, 19/22) significantly more than active NVC (41%, 16/39, $p=0.002$). None of the other parameters showed significant differences between groups (Table 3).

Sensitivity, specificity, and predictive values of OCT in the determination of PDR activity: They were, respectively 66.70%, 77.30%, 83.90% and 56.67% for the

presence of vitreous hyperreflective dots; 76.92%, 0%, 57.69% and 0% for the presence of ERM; 46.15%, 22.73%, 51.42% and 19.23% for inner retinal tissue contracture; 51.28%, 9.00%, 50% and 9.52% for vitreous invasion and for 58.97%, 86.36%, 88.46% and 54.28% for vitreous protrusion.

Intergrader agreement: The intergrader agreement for the SD-OCT features accessed was substantial with a weighted kappa of 0.64 (Standard error: 0.13, 95% CI: 0.41 to 0.94).

Discussion:

In this study, we used SD-OCT, a non-contact, non-invasive imaging technique, to describe the morphology of retinal neovascularization in PDR, with the aim of identifying specific SD-OCT signs of new vessel activity. For the purposes of this study, we designed a customized scanning protocol to better capture the NVC within the SD-OCT scan. As previously documented by Cho et al, we were successful in imaging all NVC.¹¹

Differences in SD-OCT features were observed between active and inactive NVC. Muqit et al have also recently described OCT features in PDR^{12, 13}, albeit with different descriptive terms. The present study has identified a significant higher presence of vitreous hyperreflective dots in active NVC compared to quiescent NVC with good sensibility. We hypothesize that this feature may be related to the increased vascular permeability of the NVC lesions during the active phase, leading to extravasation of sero-sanguineous components into the adjacent vitreous. We suggest that this material may lately coalesce in clusters, with hyperreflective optical properties. It should be mentioned that frank vitreous hemorrhage (VH) was not present in the image sets obtained in this study, although the presence of subclinical VH could not be completely excluded. Conversely, quiescent NVC were more commonly associated with qualitative features related to fibrotic changes. These included the presence of ERM adjacent to NVC, as well as inner retinal tissue contracture and vitreous invasion. In addition, most quiescent NVC demonstrated lesion protrusion towards the vitreous. These statistically significant findings may relate with the retraction, scarring and fibrosis that arises with the involution of the vessels after laser treatment. As in previous studies, there was a lower prevalence of

active NVC in eyes with previous panretinal laser photocoagulation.²¹

Most of the NVC included in our study had a thickened attached posterior hyaloid and were not associated with a PVD. These results are consistent with previous published studies. In a shorter series (n=16), Cho et al., reported that NVC lesions were found to arise at a vitreous attachment site, where the thickened posterior hyaloid would have served as scaffold for the growth of NVC.¹¹ Interestingly, Ono et al., concluded in a much larger prospective study (n=403) that a complete PVD seemed to be protective for the development of PDR.²² Our results are consistent with this data, given that only a small number of NVC was associated with a complete PVD (6.5%, 4/61). In keeping with this, the majority of the NVC, and especially the quiescent cases, demonstrated NVC lesions protruding towards the vitreous from the surface of the retina, as described by Cho et al as a second category of NVC.¹² Other features analyzed in this study included the presence of retinal hyperreflective dots and intraretinal cysts. Whereas these retinal hyperreflective dots have been reported to be activated microglial cells in age-related macular degeneration, in other diseases they have been described as vessel hyperpermeability products in the form of proteins or lipid deposits.^{23,24} Given the vascular abnormalities seen in PDR, the latter appears to be a sensible explanation for the findings observed. Regarding the presence of intraretinal cysts, only a quarter of the lesions presented this finding without any differences among active and inactive NVC.

The current study has a number of strengths. To our knowledge this is the first study that analyzes qualitative data from SD-OCT scans in a relatively large series of PDR eyes in an effort to identify signs of NVC activity. All OCT images were assessed by masked experienced graders with substantial intergrader agreement.

Moreover, our scanning protocol can be easily performed using standard SD-OCT devices, allowing replication of the current study in different populations. Limitations include selection bias as it was a cross-sectional study with a limited cohort recruited in two tertiary referral specialized medical retina clinics. As a result, the cases evaluated may represent more advanced PDR than those seen in a standard community setting. Also, as this was an exploratory study, our sample was insufficient to include multiple comparisons, such as cross match between vitreous and retinal features, and for appropriate test validation. It should be regarded as a hypothesis generator that needs to be confirmed in larger studies. Another important consideration is the fact that the majority of eyes (81.4%) were previously submitted to panretinal photocoagulation so it is possible that the higher incidence of ERM in the quiescent NVC group was due to the laser treatment and not to the neovascularization inactivity. Additionally, as majority of our patients did not have a PVD, we were unable to correlate the growth of NV into the vitreous with incomplete PVD. An additional limitation is the inability of SD-OCT to capture the totality of the NVC area, as seen on slit-lamp biomicroscopy. Future developments in OCT technology may overcome this limitation by allowing image capture over wider areas of the retina, as well as visualization of more peripheral retinal pathologies.

In conclusion, this study reports that commercially available SD-OCT devices can be used to assess features of NVC in patients with diabetic retinopathy. This is a relatively new field and the present study differs from previous reports as it was designed to establish whether SD-OCT can match the clinical determination of disease state. Five distinctive signs were identified as significantly different between active and quiescent NVC: presence of vitreous hyperreflective dots in active NVC and presence of epiretinal membrane, inner retinal tissue contracture, vitreous

invasion and protrusion towards vitreous in quiescent NVC. In that respect, our results suggest that OCT may be useful for distinguishing between active and quiescent NVC and may be useful with regard to clinical decision-making and monitoring response to treatment.

Interestingly, the use of the confocal scanning laser ophthalmoscope eye-tracking system employed by the SD-OCT device could allow repeated OCT scan captures in the exact location of lesions, providing an exceptional tool to monitor NVC evolution or response to treatment during follow up. With this aim further longitudinal studies including larger cohorts of patients are required to confirm these preliminary findings, as well as to evaluate their relationship with other imaging techniques such as fluorescein angiography and elucidate the real potential of this non-invasive imaging technique in assessing new vessel activity in PDR.

Figure legends:

Figure 1. (a) Colour fundus photograph of a patient with inactive NVD. (b) Late phase fundus fluorescein angiogram showing no leakage from the NVD. (c) 3D spectral-domain optical coherence tomography (SD-OCT) reconstruction of the NV complex showing its protrusion from the disc. (d) Green horizontal lines represent SD-OCT B-scans through the NVD. The NV invades the vitreous and is associated with tissue contracture, an epiretinal membrane and retinal and vitreous hyperreflective dots.

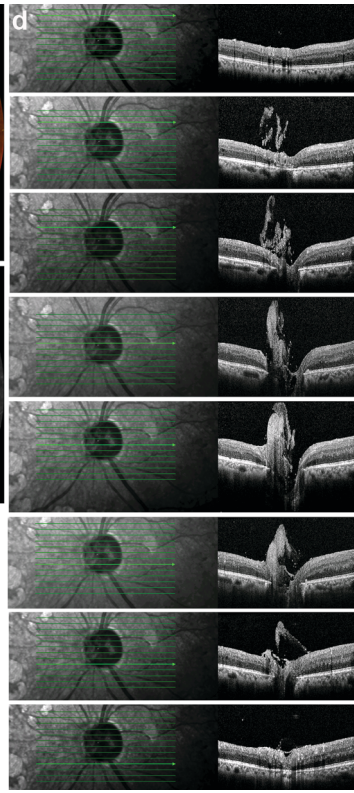
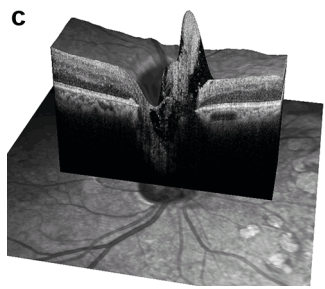
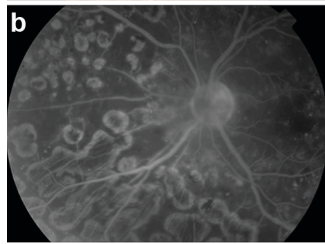
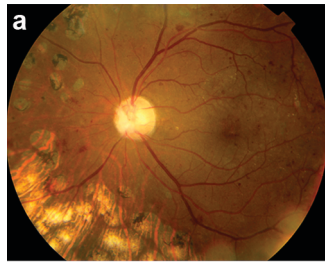
Figure 2. (i) Examples of 3D spectral-domain optical coherence tomography (SD-OCT) reconstructions of the NVE complexes, (a) active and (b-d) inactive. (ii) Examples of SD-OCT B-scans through the NV. Horizontal arrow lines represent the plane of the scan. (a) Vitreous hyperreflective dots. Flat active NVE with associated vitreous hyperreflective dots. (b) Vitreous invasion. Inactive NVE with vitreous invasion, intra-retinal cysts and features of tissue contracture. (c) Epiretinal membrane adjacent to NVC. Protruding inactive complex with an associated epiretinal membrane (ERM) and retinal hyperreflective dots (arrowheads). (d) C-shaped NV complex with ERM and features of tissue contracture.

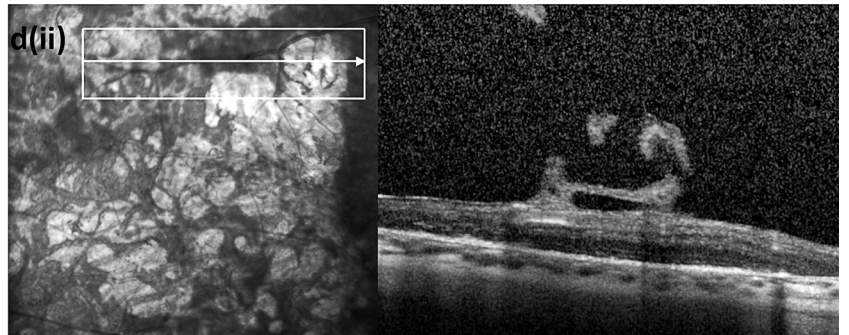
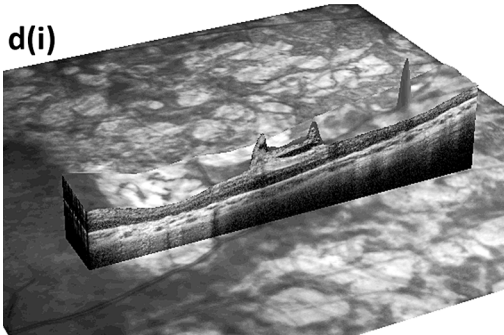
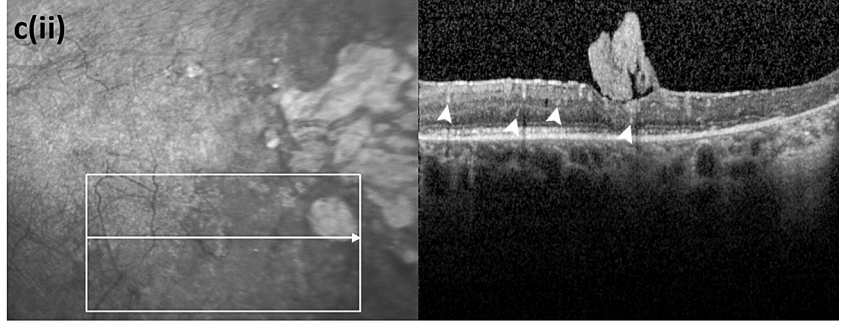
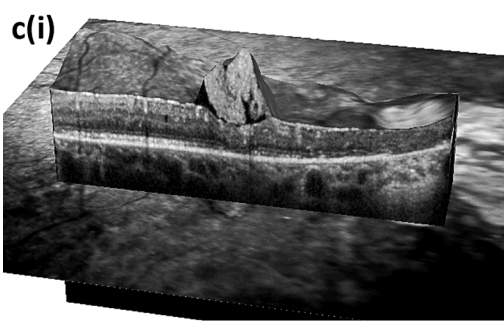
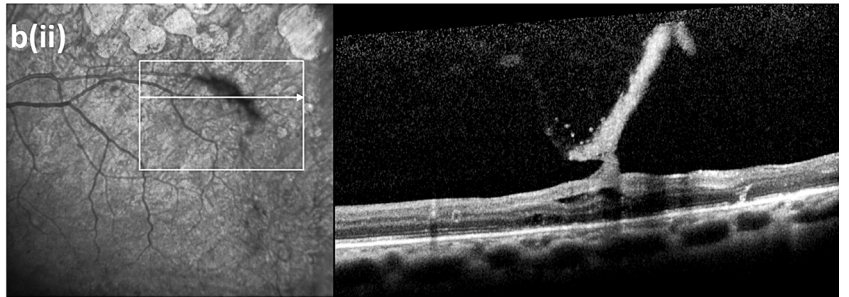
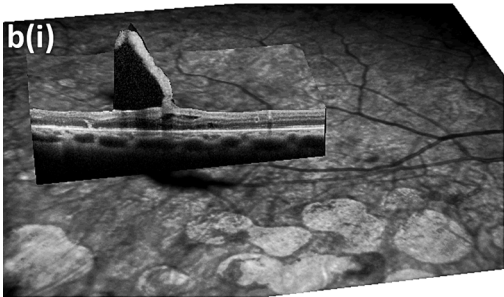
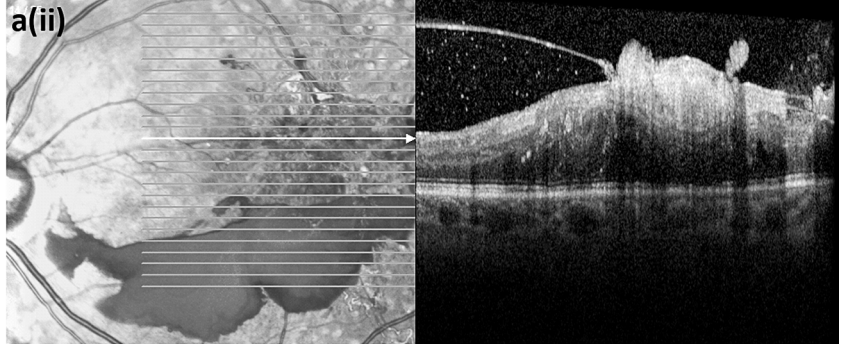
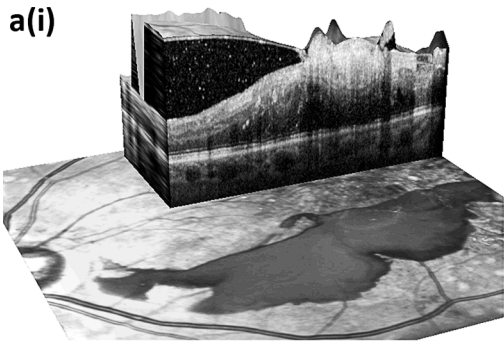
Figure 3. (a) Colour fundus photograph of a patient with active NVE. (b) Magnification of the annotated area in 2a showing the NVE in detail. (c) Early phase fundus fluorescein angiogram demonstrating temporal capillary non-perfusion and leakage from the NV complex, which (d) increased in size and intensity through the study, corresponding to active disease. (e-f) Green horizontal lines represent spectral-domain optical coherence tomography B-scans through the NVE. (e) Depicted area is enlarged and shows a flat NVE complex with vitreous invasion (red) and associated vitreous hyperreflective dots (green). (f) Magnification of the delineated area shows in more detail the dilated tips of the NVE (red) and the hyperreflective dots (green).

References:

1. Kempen JH, O'Colmain BJ, Leske MC, et al. The prevalence of diabetic retinopathy among adults in the United States. *Archives of ophthalmology* 2004;122:552-563.
2. Moss SE, Klein R, Klein BE. The 14-year incidence of visual loss in a diabetic population. *Ophthalmology* 1998;105:998-1003.
3. Grading diabetic retinopathy from stereoscopic color fundus photographs--an extension of the modified Airlie House classification. ETDRS report number 10. Early Treatment Diabetic Retinopathy Study Research Group. *Ophthalmology* 1991;98:786-806.
4. Wilkinson CP, Ferris FL, 3rd, Klein RE, et al. Proposed international clinical diabetic retinopathy and diabetic macular edema disease severity scales. *Ophthalmology* 2003;110:1677-1682.
5. Klein R, Klein BE, Moss SE, et al. The Wisconsin epidemiologic study of diabetic retinopathy. II. Prevalence and risk of diabetic retinopathy when age at diagnosis is less than 30 years. *Archives of ophthalmology* 1984;102:520-526.
6. Huang D, Swanson EA, Lin CP, et al. Optical coherence tomography. *Science* 1991;254:1178-1181.
7. Lee DH, Kim JT, Jung DW, et al. The relationship between foveal ischemia and spectral-domain optical coherence tomography findings in ischemic diabetic macular edema. *Invest Ophthalmol Vis Sci* 2013;54:1080-1085.
8. Comyn O, Heng LZ, Ikeji F, et al. Repeatability of Spectralis OCT measurements of macular thickness and volume in diabetic macular edema. *Invest Ophthalmol Vis Sci* 2012;53:7754-7759.
9. Hatem E, Khwaja A, Rentiya Z, et al. Comparison of time domain and spectral domain optical coherence tomography in measurement of macular thickness in macular edema secondary to diabetic retinopathy and retinal vein occlusion. *J Ophthalmol* 2012;2012:354783.
10. Otani T, Kishi S. Tomographic assessment of vitreous surgery for diabetic macular edema. *Am J Ophthalmol* 2000;129:487-494.
11. Cho H, Alwassia AA, Regiatieri CV, et al. Retinal neovascularization secondary to proliferative diabetic retinopathy characterized by spectral domain optical coherence tomography. *Retina* 2013;33:542-547.
12. Muqit MM, Stanga PE. Fourier-domain optical coherence tomography evaluation of retinal and optic nerve head neovascularisation in proliferative diabetic retinopathy. *Br J Ophthalmol* 2014;98:65-72.
13. Muqit MM, Stanga PE. Swept-source optical coherence tomography imaging of the cortical vitreous and the vitreoretinal interface in proliferative diabetic retinopathy: assessment of vitreoschisis, neovascularisation and the internal limiting membrane. *Br J Ophthalmol* 2014;98:994-7.
14. Lee CS, Lee AY, Sim DA, et al. Reevaluating the definition of intraretinal microvascular abnormalities and neovascularization elsewhere in diabetic retinopathy using optical coherence tomography and fluorescein angiography. *Am J Ophthalmol* 2015;159:101-10.e1.
15. Classification of diabetic retinopathy from fluorescein angiograms. ETDRS report number 11. Early Treatment Diabetic Retinopathy Study Research Group. *Ophthalmology* 1991;98:807-822.
16. Treatment techniques and clinical guidelines for photocoagulation of diabetic macular edema. Early Treatment Diabetic Retinopathy Study Report Number 2. Early Treatment Diabetic Retinopathy Study Research Group. *Ophthalmology* 1987;94:761-774.
17. Focal photocoagulation treatment of diabetic macular edema. Relationship of treatment effect to fluorescein angiographic and other retinal characteristics at baseline: ETDRS report no. 19. Early Treatment Diabetic Retinopathy Study Research Group. *Archives of ophthalmology* 1995;113:1144-1155.

18. A randomized trial comparing intravitreal triamcinolone acetonide and focal/grid photocoagulation for diabetic macular edema. *Ophthalmology* 2008;115:1447-1449, 1449 e1441-1410.
19. Mackenzie S, Schmermer C, Charnley A, et al. SDOCT imaging to identify macular pathology in patients diagnosed with diabetic maculopathy by a digital photographic retinal screening programme. *PloS one* 2011;6:e14811.
20. Landis JR, Koch GG. The measurement of observer agreement for categorical data. *Biometrics* 1977;33:159-174.
21. Neubauer AS, Ulbig MW. Laser treatment in diabetic retinopathy. *Ophthalmologica Journal internationale d'ophtalmologie International journal of ophthalmology Zeitschrift fur Augenheilkunde* 2007;221:95-102.
22. Ono R, Kakehashi A, Yamagami H, et al. Prospective assessment of proliferative diabetic retinopathy with observations of posterior vitreous detachment. *International ophthalmology* 2005;26:15-19.
23. Coscas G, De Benedetto U, Coscas F, et al. Hyperreflective dots: a new spectral-domain optical coherence tomography entity for follow-up and prognosis in exudative age-related macular degeneration. *Ophthalmologica Journal internationale d'ophtalmologie International journal of ophthalmology Zeitschrift fur Augenheilkunde* 2013;229:32-37.
24. Okubo A, Unoki K, Yoshikawa H, et al. Hyperreflective dots surrounding the central retinal artery and vein in optic disc melanocytoma revealed by spectral domain optical coherence tomography. *Japanese journal of ophthalmology* 2013;57:108-112.





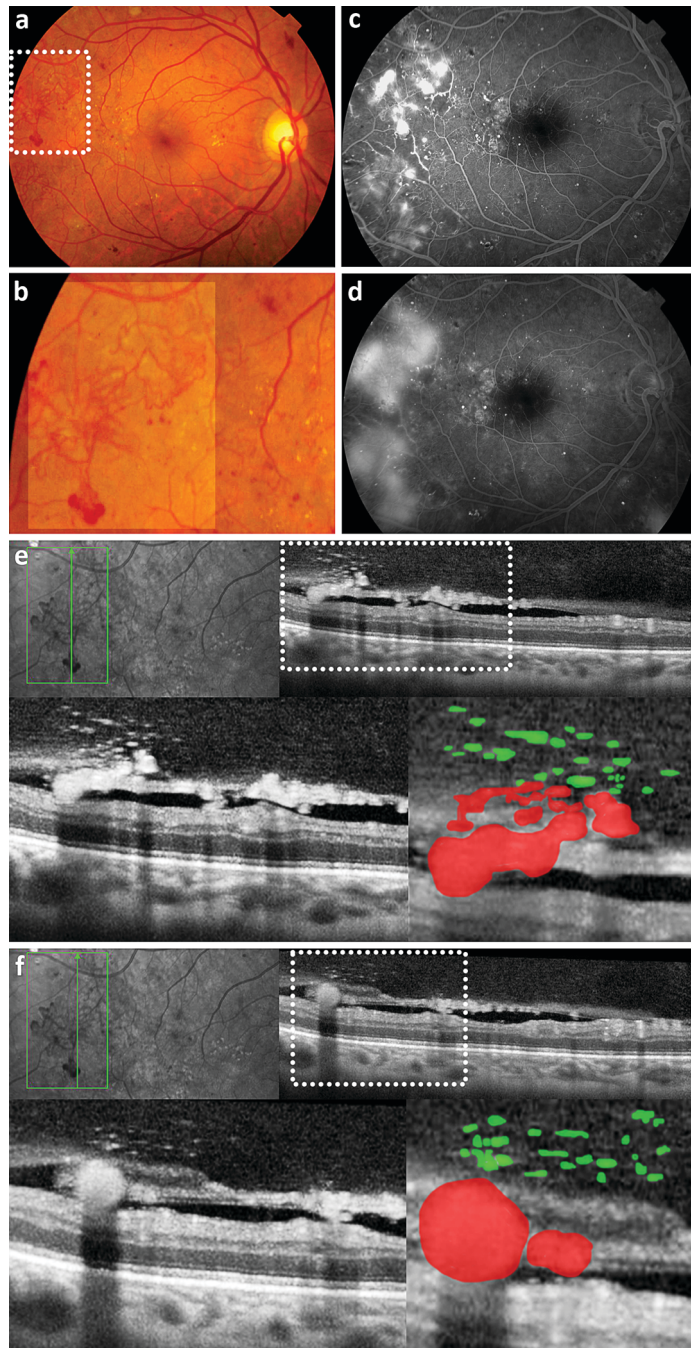


Table 1. Baseline Demographics and Clinical Characteristics of Patients with Neovascularization of the Disc and Elsewhere.

	No PRP, <i>n</i> = 6	PRP, <i>n</i> = 24
Age, y, mean (SD)	49	57.2
Gender, <i>n</i>, female/male	1/5	13/11
Type of DM, <i>n</i>, 1/2	1/5	7/17
VA, logMAR, mean (SD) OD/OS	0.27(0.25)/ 0.26(0.27)	0.27(0.24)/0.29(0.37)
CMT, μm, mean (SD) OD/OS	323.0 (36.40) / 366.5 (77.48)	292.79 (110.06) / 316.64 (86.36)
Eyes analyzed, <i>n</i>, 1/2	4/2	13/11
Type of SD-OCT scan obtained		
NVD	3	8
NVE	1	10
Both	2	6
Number of SD-OCT scans obtained		
NVD	6	17
NVE	3	35

Abbreviations: y = years; PRP = panretinal photocoagulation; DM = Diabetes Mellitus; NVD = Neovascularization of the Disc; NVE = Neovascularization Elsewhere; OD = Right eye; OS = Left eye; CMT = Central Macular Thickness; SD-OCT = Spectral-Domain Optical Coherence Tomography

Table 2. Baseline Clinical Characteristics of the Eyes with Neovascularization of the Disc and Elsewhere.

	Age (Years) (Mean [SD])	p-value	Male Sex, n (%)	p-value	Right Eye, n (%)	p-value	Type 1 or 2 DM n (%)	p-value	logMAR VA (Mean [SD])	p-value	Laser photocoagulation at the time of SD-OCT scan, n (%)	p-value	CMT (um) (Mean [SD])	p-value
Eyes														
All (n=43)	54.9 [12.3]		24 (55.8)		20 (87.0)		13 (30.2) Type 1; 30 (69.8) Type 2		0.24 [0.19]		35 (81.4)		311.3 [91.0]	
Active NVD/E (n=27)	55.7 [12.6]	0.51	18 (66.6)	0.45	13 (48.1)	0.65	6 (22.2) Type 1; 21 (77.8) Type 2	0.01*	0.24 [0.22]	0.61	20 (74.0)	0.001†	326.5 [104.8]	0.17
Inactive NVD/E (n=16)	53.4 [12.0]		6 (37.5)		7 (43.8)		7 (43.8) Type 1; 9 (56.2) Type 2		0.24 [0.13]		15 (93.8)		285.7 [55.0]	

The Chi-Squared test was used for statistical analysis of categorical and the Mann-Whitney U test for continuous variables. p values significant at 5% level are indicated with (*), and (†) at 1% level. Abbreviations: DM = Diabetes Mellitus; NVD = Neovascularization of the Disc; NVE = Neovascularization Elsewhere; SD= Standard Deviation; OD = Right eye; OS = Left eye; CMT = Central Macular Thickness; SD-OCT= Spectral Domain Optical Coherence Tomography; VA = Visual Acuity

Table 3. Assessment of SD-Optical Coherence Tomographic Features of Neovascularization of the Disc and Elsewhere

SD-OCT Features	NVD			NVE			Combined NVD/E		
	Active	Quiescent	p-value	Active	Quiescent	p-value	Active	Quiescent	p-value
	(n [%])	(n [%])		(n [%])	(n [%])		(n [%])	(n [%])	
All SD-OCT scans	15 [65,2]	8 [34,8]		24 [63,2]	14 [36,8]		39 [63,9]	22 [36,1]	
Vitreoretinal morphologic parameters									
Posterior vitreous detachment									
Yes	0 (0)	0 (0)	0,03*	1 (4,20)	3 (21,4)	0,12	1 (2,6)	3 (13,6)	0,10
No	14 (93,3)	4 (50,0)		23 (95,8)	7 (50,0)		37 (94,9)	11 (50,0)	
Thickening of the posterior hyaloid									
Yes	12 (80,0)	4 (50,0)	0,71	19 (79,2)	6 (42,9)	0,81	31 (79,5)	10 (45,5)	0,68
No	2 (13,3)	2 (25,0)		5 (20,8)	2 (14,3)		7 (17,9)	4 (18,1)	
ERM at NVC									
Yes	11 (73,3)	8 (100)	0,30	19 (79,2)	14 (100)	0,18	30 (76,9)	22 (100)	0,04*
No	4 (26,7)	0 (0)		5 (20,8)	0 (0)		9 (23,1)	0 (0)	
Vitreoretinal traction									
Yes	5 (33,3)	5 (62,5)	0,37	3 (12,5)	4 (28,6)	0,13	8 (20,5)	9 (40,9)	0,16
No	10 (66,7)	3 (37,5)		21 (87,5)	10 (71,4)		31 (79,5)	13 (59,1)	
Hyperreflective dots in the vitreous									
Yes	9 (60,0)	2 (25,0)	0,25	17 (70,8)	3 (21,4)	0,009†	26 (66,7)	5 (22,7)	0,002†
No	6 (40,0)	6 (75,0)		7 (29,2)	11 (78,6)		13 (33,3)	17 (77,3)	
Retinal morphologic parameters									
Retinal tissue contracture									
Yes	10 (66,7)	8 (100)	0,19	8 (33,3)	9 (64,3)	0,13	18 (46,2)	17 (77,3)	0,03*
No	5 (33,3)	0 (0)		16 (66,7)	5 (35,7)		21 (53,8)	5 (22,7)	
Intraretinal cysts									
Yes	2 (13,3)	0 (0)	0,76	7 (29,2)	6 (42,9)	0,50	9 (23,1)	6 (27,3)	0,88
No	13 (86,7)	8 (100)		17 (70,8)	6 (42,9)		30 (76,9)	14 (63,6)	
Retinal hyperreflective dots									
Yes	8 (53,3)	3 (37,5)	0,78	18 (75,0)	9 (64,3)	0,99	26 (66,7)	12 (54,5)	0,65
No	7 (46,7)	5 (62,5)		6 (25,0)	4 (28,6)		13 (33,3)	9 (40,9)	
NVC morphologic parameters									
Reflectivity of NVC									
High	7 (46,7)	3 (37,5)	0,98	12 (50,0)	6 (42,9)	0,93	19 (48,7)	9 (40,9)	0,59
Medium	8 (53,3)	5 (62,5)		12 (50,0)	8 (57,1)		20 (51,3)	13 (59,1)	
Shadowing outer retina									
Yes	12 (80,0)	8 (100)	0,48	24 (100)	11 (78,6)	0,08	36 (92,3)	19 (86,4)	0,76
No	3 (20,0)	0 (0)		0 (0)	3 (21,4)		3 (7,7)	3 (13,6)	
Vitreous invasion									
Yes	6 (40,0)	8 (100)	0,02*	14 (58,3)	12 (85,7)	0,16	20 (51,3)	20 (90,9)	0,02*
No	9 (60,0)	0 (0)		10 (41,7)	2 (14,3)		19 (48,7)	2 (9,1)	
Relative position of NVC									
Flat	7 (46,7)	1 (12,5)	0,24	16 (66,7)	2 (14,3)	0,005†	23 (59,0)	3 (13,6)	0,002†
Protruding	8 (53,3)	7 (87,5)		8 (33,3)	12 (85,7)		16 (41,0)	19 (86,4)	

The Fisher's exact test was used for statistical analysis of categorical variables in eyes with NVD, and the Chi-Squared test in eyes with NVE. The two-tailed t-test was used for continuous variables in all eyes. p values significant at 5% level are indicated with (*), and (†) at 1% level. Abbreviations: NVC= New Vessel Complex; NVD = Neovascularization of the Disc; NVE = Neovascularization Elsewhere; SD-OCT = Spectral-Domain Optical Coherence Tomography; ERM = epiretinal membrane